Universiteit
Leiden
The Netherlands

Imaging plasma membrane domains in signal transduction pathways

Pezzarossa, A.

Citation

Pezzarossa, A. (2012, March 13). *Imaging plasma membrane domains in signal transduction pathways*. Retrieved from https://hdl.handle.net/1887/18585

Version:	Not Applicable (or Unknown)
License:	Leiden University Non-exclusive license
Downloaded from:	https://hdl.handle.net/1887/18585

Note: To cite this publication please use the final published version (if applicable).

Cover Page

Universiteit Leiden

The handle http://hdl.handle.net/1887/18585 holds various files of this Leiden University dissertation.

Author: Pezzarossa, A.
Title: Imaging plasma membrane domains in signal-transduction pathways
Issue Date: 2012-03-13

Chapter 5

Microsecond tracking in living cells[1]

Interaction of proteins with nanometers sized structures in the plasma membrane takes place on the microsecond time scale. However, until recently this regime was not accessible experimentally because of technical limitations of fluorescence microscopy. Here we report on the application of μsSMT to study the mobility of a GPI-anchored protein in living U2OS cells. We combine the high temporal resolution of our recently developed microsecond tracking technique with a novel, highly specific genetic labeling technique, complementation-activated light microscopy (CALM). A protein fusion with a split-GFP system is used to target the GPI-anchor that is stably expressed in cells, and through complementation with a synthetic fluorescent M3 peptide a double labeling is achieved. Our results show evidences of confinement in nanometer sized domains at the time scale of 500 μs.

[1]This chapter is based on: Pezzarossa, A., Pinaud, F., Schmidt,T. "Is there evidence for hop-diffusion? GPI-anchor protein diffusion at microsecond time-scale." (in preparation)

5.1 Introduction

The spatial structure and organization of the plasma membrane is highly relevant for the behavior of biomolecules in living cells. In recent years, evidence from both biochemical experiments and light microscopy proved that the plasma membrane is a highly complex environment, organized in compartments that varies in size from a few tens to a few hundreds of nanometers (1). The local environment affects the mobility of proteins embedded in the membrane matrix, and deviations from free Brownian diffusion have been observed for many transmembrane and membrane-anchored proteins (3). Single-particle tracking has been the ideal tool to study protein mobility, but its low time resolution (few tens of milliseconds) has proven to be a limit to study the fast interaction with smaller domains, characterized by a sub-millisecond time-scale. Tracking at 25 μs time resolution have been performed previously by Kusumi's group, using colloidal gold nano-probes (4, 5), yielding a model for hop-diffusion in which particle are temporarily trapped for 1 to 10 ms in corrals of typical size of 200 nm. However, these experiments suffer from non-specific binding and the big size of the gold nano-probes, which can affect the motion of the proteins.

In particular, a set of proteins characterized by the presence of a glycosyl-phosphatidyl-inositol-anchored (GPI-anchored) motif, have been associated with membrane microdomains enriched in cholesterol and and glycosphingolipids. These studies (8) showed that the GPI-anchoring sequence of the human CD14 receptor alone is targeted to microdomains. Pinaud et al. demonstrated that the GPI-anchor mobility is characterized by the presence of a fast and a slow diffusing subpopulations, and proposed a dynamical partitioning between microdomains and the rest of the membrane. However, due to the limited time-resolution it was not possible to verify whether the observed behavior was due to hop-diffusion of the proteins in and out of the domains.

Recently, we reported on a technique to track single-particles down to a few μs, microsecond single-molecule tracking (μsSMT), using a double dye label (6). Here we apply μsSMT to study the mobility of a GPI-anchored protein in living U2OS cells, down to 500 μs. We aim at learning more about the molecular organization and the dynamic interaction within nanodomains. To reliably label the protein of interest we applied complementation-activated light microscopy (CALM) (7). A genetically encoded split-GFP was fused to the GPI-anchoring signal peptide of the

human CD14 receptor (8). Through spontaneous self-complementation of the split-GFP with the a synthetic peptide conjugated to Alexa 647 fluorophore we achieved the double label necessary for μsSMT. The GPI-anchor was tracked down to 500 μs. Analysis of the mean squared displacement (MSD) of the protein confirms the previous observation that the GPI-anchor interacts with membrane domains. Here, we resolve this interaction with unprecedented time resolution, and these observations seems to confirm the existence of hop-diffusion, suggested by Kusumi et al. (5) using tracking of μm-sized gold beads earlier.

5.2 Material and methods

5.2.1 Cell culture

Stably transfected human osteosarcoma cells (U2OS)(7) were cultured in DMEM medium supplemented with 10% fetal calf serum (FCS), streptomycin (200 μg/ml) and penicillin (200 U/ml) in a 7% CO2 humidified atmosphere at 37 °C (95% humidity). Cells were transferred every 4 days. For microscopy, cells were cultured on 25 mm $\oslash$ glass slides, pretreated with hydrogen fluoride.

5.2.2 Split-GFP complementation

Peptide complementation was performed following the protocol by Pinaud (7). Briefly, cells grown to $\sim$70% confluence were incubated for 30 minutes with 50 μM M3-Alexa647 peptide solution in Tyrode's buffer, supplemented with 2 mM Trolox (Sigma). After incubation, cells were washed 5 times with Tyrode's buffer. Incubation was performed on ice to prevent internalization of the protein.

5.2.3 Single-molecule microscopy

The single-molecule setup has been previously described (2). Here it was modified to allow for total internal reflection (TIRF) detection. Briefly, the microscope (Axiovert 100; Zeiss) was equipped with a 60$\times$ oil-immersion objective (NA=1.45, Olympus). The samples were illuminated for $t_{\mathrm{ill}} =$ 3 ms, by an Ar^+ laser (Spectra Physics) with a wavelength of 488 nm and a diode laser (Power technology) with a wavelength of 639 nm. The length of the laser pulses t_{ill} and the time lag between the pulses Δt

were set by an acousto-optical tunable filter (AOTF) (AA Electrooptique). An appropriate filter combination (dichroic FF497-661 and emission filter Z515/647m, Chroma Technology) permitted the detection of individual fluorophores by a liquid nitrogen cooled slow-scan CCD camera system (Princeton Instruments). A dichroic wedge split the emitted light to two different regions of the CCD according to the emission wavelength. In this way the fluorescence signals from the GFP and Alexa647 were spatially separated on the CCD.

5.2.4 Correction for chromatic aberration

Since the signals from the two fluorophores had to be correlated, correction for chromatic aberration had to be applied. To establish the correspondence between the two signals we used fluorescent beads (200 nm TetraSpeck beads, Invitrogen) which were observable in both channels. The beads were adsorbed to a coverslip and moved through the whole region of interest. The positions of the bead in the two channels and the shift matrix was built as described in reference (6). The beads were imaged prior to measurements on cells.

5.2.5 Data analysis

Data were analyzed using particle-image cross-correlation spectroscopy (PICCS) (6). PICCS calculates the cross-correlation function $C_{\mathrm{cum}}(r^2, \Delta t)$ between two different signals (further termed "green" and "red"). In μsSMT, Δt is the time-lag between the illumination of the two probes. $C_{\mathrm{cum}}(r^2, \Delta t)$ is equal to the average number of green signals at time $t+\Delta t$ which have a distance smaller than r to a certain red signal at time t. As discussed in (9), $C_{\mathrm{cum}}(r^2, \Delta t)$ corresponds to the cumulative probability $P_{\mathrm{cum}}(r^2, \Delta t)$, plus a corrective factor which accounts for random correlation of the molecules:

$$C_{\mathrm{cum}}(r^2, \Delta t) = \beta_{\mathrm{g}} P_{\mathrm{cum}}(r^2, \Delta t) + c_{\mathrm{red}} \pi r^2 \tag{5.1}$$

Here β_{g} is the correlation fraction, and πc_{red} is the density of red signals. These parameters are determined by fitting a straight line to the linear part of $C_{\mathrm{cum}}(r^2, \Delta t)$ plotted against r^2.

In the experiments presented $P_{\mathrm{cum}}(r^2, \Delta t)$ is best fitted according to a two-population model:

$$P_{\mathrm{cum}}(r^2, \Delta t) = 1 - \left[\alpha \exp\left(-\frac{r^2}{4D_1\Delta t}\right) + (1-\alpha)\exp\left(-\frac{r^2}{4D_2\Delta t}\right)\right] \quad (5.2)$$

5.3 Results

5.3.1 System characterization

The split-GFP-GPI anchor system is composed of two non-fluorescent fragments with large difference in size, as reported in (8). For microsecond tracking, the small fragment (M3 peptide) has been conjugated to a Alexa647 dye, through a cysteine modification (see reference (8) for details). The large fragment consist of a full length GFP minus the M3 fragment. When incubated in solution together, the two fragments refold to form a fluorescent GFP. The absorption and emission spectra of the complemented split-GFP and the Alexa 647 dye show poor spectral overlap (see figure 5.1a). However, due to the small distance between the red fluorophore and the green chromophore, $R_0 = 3.6$ nm, energy transfer between the two can occur. The system was characterized previously in bulk (7), showing that indeed fluorescence resonance energy transfer (FRET) occurs. Further, the system was studied at single-molecule level in solution using cross-correlation spectroscopy (FCCS). FCCS experiments were performed at a concentration of 250 pM using 488 nm excitation and dual detection of GFP and Alexa 647. A cross-correlation signal was observed (see figure 5.1b), clearly indicating the occurrence of 25%FRET. The diffusion coefficient of the complemented GFP, as determined by FCCS, is equals to what predicted for GFP in solution ($D = 68 \pm 5$ μm^2/s) (Pinaud, private communication).

For μsSMT it is required that the two signals are independent. Thus, processes like energy transfer and cross-talk need to be minimized. In our experiments the two fluorophores were firmly attached to a membrane protein, and their rotational freedom is reduced. Thus, the high FRET value observed in solution might be highly reduced, and further system characterization was needed.

The cell sample was complemented with the M3 peptide as described in section 5.2.2. The sample was illuminated for $t_{\mathrm{ill}} = 3$ ms with 488 nm only. Individual molecules were localized in both the green and the red image, and correction for chromatic aberration was subsequently applied. First we quantified the amount of green and red signal detected: as shown

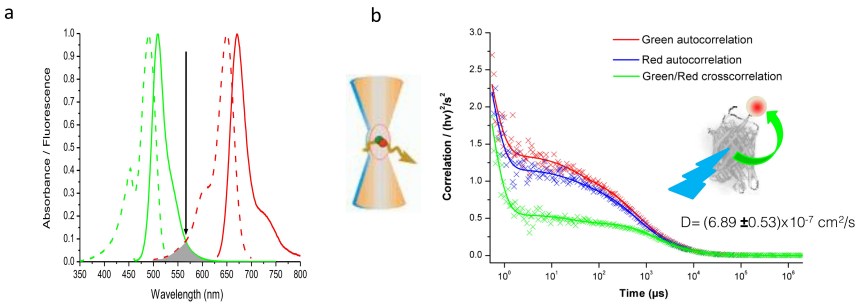

Figure 5.1: Characterization of the split-GFP-Alexa647 system in solution. **a)** Absorption (solid lines) and emission (dotted lines) spectra of complemented split-GFP (green) and Alexa647 (red). The two spectra are poorly overlapping. **b**Fluorescence cross-correlation experiments on complemented split-GFP-M3-Alexa647. From fitting of the data 25% of FRET between the GFP cromophore and Alexa647 was estimated. (Figures by Fabien Pinaud, private communication)

in figure 5.2 a, $\sim$ 5000 peaks were found in the green channel, while only 1368 were detected in the red channel. Intensity and width distribution of the signals in both channels confirmed our prediction that we were observing individual molecules (see figure 5.2 b-c). From the number of observed signals on 488 nm-excitation we have to conclude that $\sim$ 27% of GFP signals results in a signals in the red channel. This cross-talk does account for both FRET and optical cross-talk between the two channels due to imperfect optical separation of the emitted signals. This number is comparable to the FRET efficiency observed in solution. However, for μsSMT only signals that are cross-correlated between the two images will enter the analysis (i.e. only molecules with FRET efficiency $\sim$ 50% will be taken into account), while other signals will be discarded. To evaluate the background level of cross-correlation, we evaluated the cumulative probability function C_{cum}. The intersection of the y-axis obtained by fitting of the linear part of C_{cum} quantifies the level of cross-correlation. Here we found that only 3% of the green signals were correlated with red ones as shown in figure 5.2.

5.3.2 Microsecond mobility of GPI-anchor

To study the mobility of the GPI-anchor and its possible interaction with membrane structures we applied μsSMT. This minimal GPI-construct we

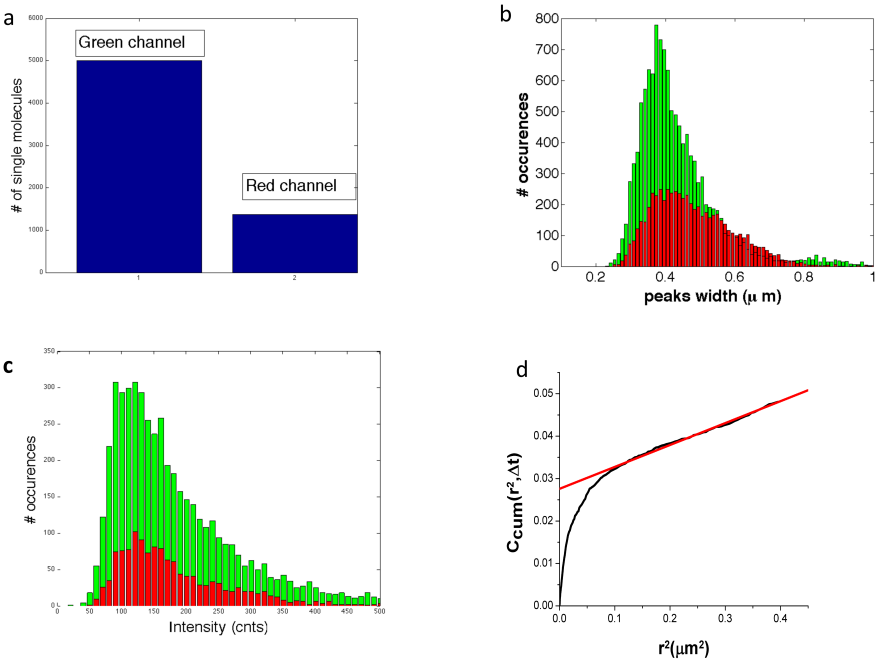

Figure 5.2: Evaluation of cross-talk and FRET of the spilt GFP-M3Alexa647 system in cells. Data acquired with 488 nm excitation only.**a)** Total amount of green and red molecules detected. $\sim 27\%$ of green molecules results in a red signal. **b-c)** Histogram of the distribution of peaks width and emission intensity for both green and red channel confirmed we were detecting single molecules. **d)** C_{cum} calculated for the data acquired with excitation at 488 nm only. 3% of cross-talk is deduced from intersection of the linear fit with the y-axis.

used here has no biological function nor specific interaction with membrane components, as already reported in (8), such that only membrane-mediated interactions could occur. The split-GFP-GPI was complemented as described in 5.2.2, and imaged for up to 500 consecutive images. The imaging area for each channel was set to 6.6×6.6 μm^2. The sample was illuminated with both 488 nm and 647 nm laser light, and the illumination time was set to $t_{\text{ill}} = 3$ ms. The delay between the green and the red channel was set to $\Delta t = 0, 0.5, 1, 3$ and 5 ms for subsequent sets of experiments. Prior to each set, a bead was scanned through the imaging area for an updated chromatic aberration correction.

Cumulative probability function was calculated, and from fitting of

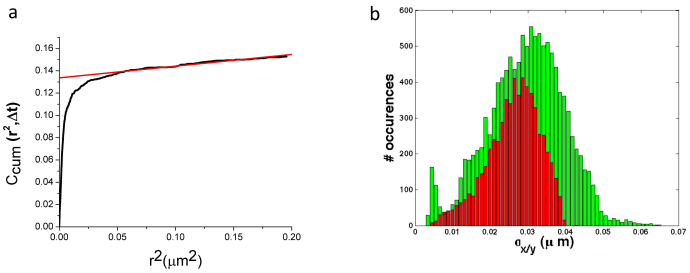

Figure 5.3: a) Evaluation of the cross-correlation fraction from fitting of linear part of C_{cum}. Intersection with y-axis gives the amount of cross-correlated signals, $\beta_{\text{g}} = 15\%$. **b)** Distribution of positional accuracy for the red and green channel, both centered ~ 30 nm

.

the linear part we retrieved the fraction of cross-correlated signal, yielding $\beta_{\text{g}} = 15\%$, as in figure 5.3 a. The fraction of cross-correlated signals is greatly higher than what was observed during control experiments using 488 nm excitation only, thus confirming the validity of the split-GFP system for μsSMT experiments.

Initially, we measured with $\Delta t = 0$ ms time-delay to asses the constant offset σ_0 in our measurement. Given that the precision with which we can measure the position of the molecules is finite, even after correction there is an apparent displacement between the two channels. We can estimate this offset by evaluating the MSD at $\Delta t = 0$ ms. The MSD was calculated from correction of C_{cum} for random correlated signal. The resulting cumulative probability function P_{cum} was best fitted with a two-fraction model (see equation 5.2), with fitting parameters α, MSD_1 and MSD_2. The presence of two populations at $\Delta t = 0$ ms, although surprising, can be explained taking into account the limited precision in measuring single-molecule positions. Since each fluorophore is localized with different precision, the positional accuracy is not a constant, but rather a distribution centered around $\sigma = 30$ nm, as shown in figure 5.3 b (10). Hence, in the fitting of P_{cum} there is an extra term to take into account. When $MSD(\Delta\text{t}) \gg 4\sigma^2$, this extra term becomes negligible, but at sub-ms time scale it is relevant. We calculated the offset as the weighted MSD of the two fractions: $\sigma_0 = \text{MSD}(\Delta t) = \alpha(MSD_1) + (1-\alpha)(MSD_2) = 0.01\ \mu\text{m}^2$.

The MSD graph resulting from measurements at $0.5 - 1 - 5$ ms is shown in figure 5.4. Each point is plotted after subtraction of the offset

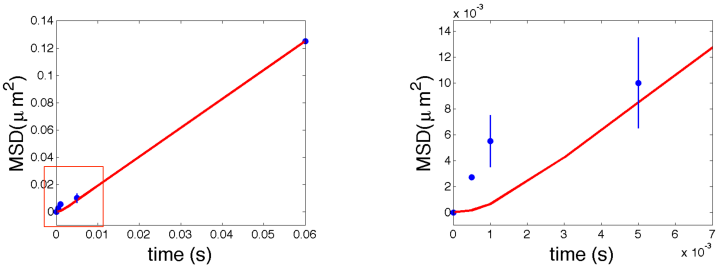

Figure 5.4: Left: MSD graph for GFP-GPI anchor protein. Data were acquired at $\Delta t = 0 - 0.5 - 1 - 5$ ms. Data point at 60 ms was measured by Pinaud. Red line: calculated MSD for GPI with diffusion coefficient $D = 0.53\ \mu\text{m}^2/\text{s}$. Right: zoom in the area at shorter time-lags (delimited by the red square on the left). The calculated curve match the results obtained for $\Delta t = 5\ ms$. For shorter time-lag a large deviation from the calculated value is observed.

σ_0. For comparison we also plotted the results for 60 ms experimentally obtained by Pinaud (8). Data are compared to the expected curve for free diffusing molecules with the diffusion coefficient of a GPI-anchor reported in literature $D = 0.53\ \mu\text{m}^2/\text{s}$. For time-lags longer than the illumination time $\Delta t > 3$ ms, the measured data point fall within the expected range. At time-lags shorter than 3 ms, instead we observe a deviation from free diffusing behavior. Fitting of the data with a free diffusion model yielded a diffusion coefficient $D > 1\mu\text{m}^2/\text{s}$. One possible explanation for the observed discrepancy between the behavior at long and short time-lags is that the protein is interacting with membrane structures at very short time scale, resulting in an apparent increased diffusion coefficient. At longer time-lag this interaction is not observable anymore, thus the MSD is best described by a free diffusing model.

5.4 Discussion

The interaction of membrane proteins with nanometer sized structures has been extensively studied using a plethora of techniques, but a common view on these interactions is still lacking. An attractive model, the so called hop-diffusion model, suggests that proteins can temporarily interact at short time scale with small corrals, and subsequently "hop" to the adjacent one (4). This model has been frequently advocate, but never directly shown. Evidences came from single-molecule tracking experiments at time resolution of 25 μs using colloidal gold nano-probes, but these results have

never been reproduced (5). Since colloidal probes could induce artifacts, it would be of high relevance to perform tracking at a time scale of few μs using small dyes. Moreover, in recent years, the group of Schütz (11) proved with theoretical and experimental evidences that sub-millisecond resolution is needed to observe molecules undergoing hop-diffusion.

In our lab we recently developed a technique to follow single-molecules with microseconds time resolution, which requires a double, spectrally separated label on the molecule of interest. In the current study we combined our μsSMT with complementation-activated light microscopy (CALM), a technique which ensure the required 1:1 green-red stoichiometry. Characterization of the system at single-molecule level showed that upon 488 nm excitation only $\sim 3\%$ of the complemented GFP signal has an associated red signal arising from FRET and/or cross talk. Upon double excitation with 488 and 647 nm, instead, the fraction of cross-correlated signal rises to $\sim 15\%$. This results confirms that CALM is the ideal technique to employ for μsSMT, given the low level of unspecific correlated signal compared to the specific one.

Subsequently, we studied the diffusion behavior of the GFP-GPI anchor in the membrane of living cells. We showed that at time-lags longer than 3 ms the protein behaved according to free diffusion, with a characteristic diffusion coefficient $D = 0.53\ \mu\text{m}^2/\text{s}$, in agreement with previous long-timescale observations (8). However, at time scale lower than 3 ms, the molecule deviated from free diffusion, showing a super-linear behavior instead. It is tempting to associate the behavior at short time scale as a temporary, short lived, trapping with small-scale corrals. It has been showed by Pinaud before that the GFP-GPI is targeted to raft-like membrane domains, enriched in the ganglioside GM1 (8).

The authors in (8) further observed two populations of GPI, characterized by different diffusive behavior. In our experiments, for extremely short time scale, the two populations are too closely spaced to be clearly resolved given our limited positional accuracy. However, in the paper it is also argued that extensive interaction of GPI with a dense network of nano-domains could be the cause of the observed slowing down. Here, although we cannot rule out the presence of two populations, we can confirm that there is interaction with nano-domains at short time scale, which is not observable at longer time-lags.

To conclude, our techniques combined with CALM proved to be an important tool to study dynamics at high time resolution. These allowed

direct observation of interaction at short time scale, which are hidden at longer times. Further improvement in molecules localization (e.g. substituting GFP with YFP, which is a far better chromophore for single-molecule fluorescence) and theoretical modeling of hop-diffusion at μs time scale will be useful to confirm our results as well as to provide a more complete picture of the interactions happening in the plane of the cell membrane.

Bibliography

[1] Lommerse, P. H. M., Spaink, H.P., Schmidt, T. (2004) In vivo plasma membrane organization: results of biophysical approaches. *Biochem. et Biophys. Acta*, **1664**, 119-131.

[2] Harms, G. S., Cognet, L., Lommerse, P. H., Blab, G. A., Schmidt, T. (2001). Autofluorescent proteins in single-molecule research: Applications to live cell imaging microscopy. *Proc. Nat. Acad. Sci.* **80**, 2396 - 2408.

[3] Saxton, M. J., Jacobson, K. (1997) Single-particle tracking: applications to membrane dynamics. *Annu. Rev. Biophys. Biomol. Struct.* **26**, 373-399.

[4] Fujiwara, T., Ritchie, K., Murakoshi, H., Jacobson, K., Kusumi, A. (2002) Phospholipids undergo hop-diffusion in compartmentalized cell membrane. *J. Cell. Biol.* **157**, 1071-1081.

[5] Murase, K., Fujiwara, T., Unemura, Y., suzuki, K., Iino, R., Yamashita, H., Saito, M., Murakoshi, H., Kusumi, A. (2004) Ultrafine membrane compartment for molecular diffusion as revealed by single molecule techniques. *Biophys. J.* **86**, 4075-4093.

[6] Semrau, S., Pezzarossa, A., Schmidt, T. (2011) Microsecond Single-Molecule Tracking (μsSMT). *Biophys. J.*, **100**, L19-21.

[7] Pinaud, F., Dahan, M. (2011) Targeting and Imaging Single Biomolecules in Living Cells by Complementation-Activated Light Microscopy with Split-Fluorescent Proteins. *Prot. Nat. Acc. Sci.* **108**, E201-E210.

[8] Pinaud, F., Michalet, X., Gopal, I., Margeat, E., Moore, H.-P., Weiss, S. (2009) Dynamic partitioning of Glycosyl-Phosphatidylinositol-Anchored protein in glycosphingolipids-rich microdomains imaged by single-quantum dot tracking. *Traffic* **10**, 691-712.

[9] S. Semrau and T. Schmidt. (2007) Particle image correlation spectroscopy (pics): Retrieving nanometer-scale correlations from high-density single-molecule position data. *Biophis. J.*

[10] Freek van Hemert, PhD thesis. Chapter 3.Casimir PhD series 2009-20. ISBN 987-90-8593-065-5. **92(2)**, 613-621.

[11] Wieser, S.; Moertelmaier, M.; Fuertbauer, E.; Stockinger, H.; Schütz, G. J. (2007) (Un)confined Diffusion of CD59 in the Plasma Membrane Determined by High-Resolution Single-Molecule Microscopy. *Biophys. J.*, **92**, 3719-28.